Sarkar, D., Kumar, M. R., Saul, J., Kind, R., Raju, P. S., Chadha, R. K., Shukla, A. K. (2003): A receiver function perspective of the Dharwar craton (India) crustal structure. - Geophysical Journal International, 154, 1, pp. 205—211.

DOI: http://doi.org/10.1046/j.1365-246X.2003.01970.x

Geophys. J. Int. (2003) **154,** 205–211

A receiver function perspective of the Dharwar craton (India) crustal structure

Dipankar Sarkar,[1] M. Ravi Kumar,[1] Joachim Saul,[2] Rainer Kind,[2] P. S. Raju,[1] R. K. Chadha[1] and A. K. Shukla[3]

[1] *National Geophysical Research Institute, Hyderabad* 500007, *India*
[2] *GeoForschungs Zentrum, Telegrafenberg,* 14473 *Potsdam, Germany*
[3] *India Meteorological Department, New Delhi* 110003, *India*

Accepted 2003 February 25. Received 2003 January 6; in original form 2002 May 13

SUMMARY

Teleseismic data from six broad-band stations on the south Indian shield have been analysed, primarily to examine the differences in the crustal structure between the eastern and western units of the Archaean Dharwar craton. *SV* receiver functions for these stations have been computed and modelled down to the Moho level in terms of Poisson's ratio and shear wave velocities. Results show that the crust for the entire Dharwar craton is mainly simple, and has a low (about 0.25) Poisson ratio. It is usually thinner and less complex than the adjacent Proterozoic crust. However, the western Dharwar craton crust (thickness ∼41 km) with a gradational Moho boundary, is substantially (>7 km) thicker than its eastern counterpart (thickness ∼34 km). No substantial differences in average crustal *S* velocities (3.6–3.8 km s^{-1}) were found. The eastern Dharwar crust below the Proterozoic Cuddapah basin was also found to have remained relatively simple and undisturbed. The continental margin to the west of the Dharwar craton appears to have shifted further west off the coast, where a possible west coast fault has down-thrown a continental crustal block under the seas. The crust constituting the Deccan volcanic province in the western Indian shield is found to be similar to that of the eastern Dharwar craton. The crust underneath the neighbouring Godavari graben is significantly different from the Dharwar crust and resembles that of a typical rift-valley.

Key words: crustal structure, Dharwar craton, Poisson's ratio, receiver functions, shear velocities.

1 INTRODUCTION

Peninsular India is a region marked by early Archaean cratonization with associated Proterozoic mobile belts. The various geological divisions (Fig. 1) are primarily of later origin, which might have affected the crustal configuration and composition. Efforts have been made, mostly by deep seismic experiments, to decipher the crust in terms of its velocity and thickness. 2-D *P*-velocity models have been put forward for different profiles shot on various geological units of the Peninsular shield (Kaila & Krishna 1992; Mahadevan 1994; Reddy *et al.* 1999). The results are of variable quality depending upon the type of experiment (refraction/wide angle/near vertical reflection), the quality of the data (analogue/digital), the processing tools (kinematic/dynamic), types and number of phases used to constrain the models, etc.

The various refraction/reflection estimates available do not bring out any clear correlation of the shield crustal structure with geological provinces, even though some inferences in this direction based on limited observations have been made, particularly in respect of the two divisions of the Dharwar craton (Reddy *et al.* 2000), the western Dharwar craton (WDC) and the eastern Dharwar craton (EDC). Two decades ago, the possibility of different crustal thickness in the two divisions was geologically postulated by Swaminath & Ramakrishnan (1981) by examining the differences in grades of metamorphism in rocks on either side of the meridional Closepet granites, which divides the Dharwar craton.

Earlier, receiver function analysis of Indian shield data brought out largely simpler and thinner Indian Archaean crust, as against complex and thicker crust in the Proterozoic belts (Kumar *et al.* 2001). For DVP also, a relatively thin crustal thickness was reported in conformity with the results from refraction studies (Kaila *et al.* 1981). However, due to the absence of stations on the Dharwar craton (except HYB on EDC), it was not possible to comment upon intracratonic variation in crustal thickness. With the installation of additional broad-band stations in 1999, more data have become available, particularly from the Dharwar craton. This gives us an opportunity to examine the Dharwar crust in detail, in order to find differences in the crustal structure between these two blocks. In this paper, we analyse the data from the broad-band stations sited on the Dharwar craton and the adjoining Godavari graben, apply the receiver function technique to decipher the crustal velocity structure,

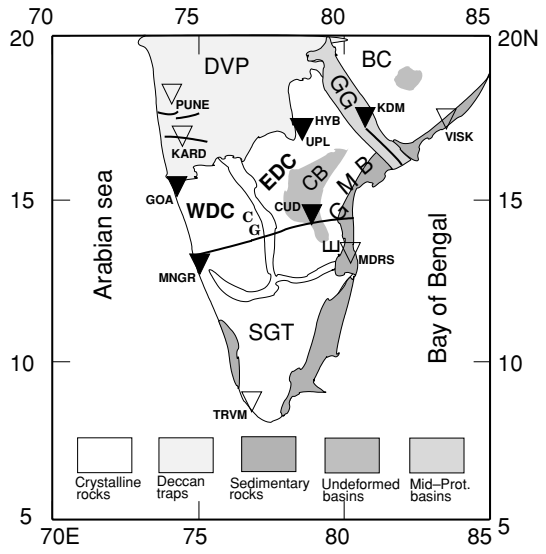

Figure 1. Distribution of broad-band stations on different geological units of southern India (adapted from Goodwin 1996). Stations used in the present analysis are shown as filled triangles, others are shown unfilled. Refraction/wide-angle reflection survey lines are also shown. EDC: Eastern Dharwar Craton, WDC: Western Dharwar Craton, CG: Closepet Granites, CB: Cuddapah Basin, DVP: Deccan Volcanic Province, GG: Godavari Graben, BC: Bhandara craton, SGT: Southern Granulite Terrain, EGMB: Eastern Ghat Mobile Belt.

and examine the possible intracratonic differences and compare the results with those from adjacent provinces.

2 GEOLOGY

The Dharwar craton and the granulite terrain are the principal constituents of the south Indian shield, for which two southward-converging faulted sides are bounded by the seas. The Dharwar craton includes numerous submeridional Dharwar and Kolar schist belts that unconformably overlie the peninsular gneissic complex (Swaminath *et al.* 1976). This craton is composed of the oldest rocks (3.4 Ga) found on Earth. A major crust-forming event stabilized the peninsular gneiss of south India at 3.0 Ga. Another major crust-forming event characterized by high-grade metamorphism consolidated the southern shield at 2.5 Ga. This event was preceded by the formation of the 350 km long Closepet granites cutting across the Dharwar metasupracrustal rocks. Large-scale mixing occurred between the magmatic and crustal melts, giving rise to the Closepet granite complex (Goodwin 1996; Naqvi & Rogers 1996).

The Dharwar craton has been divided into western and eastern parts approximately along the western margin of the Closepet granites. Intermediate pressure metamorphism in the western Dharwar craton, and low-pressure metamorphism in the eastern Dharwar craton, associated with the Archaean tectonic event, affected the supracrustal rocks and gneisses. This provided a setting for the development of paired metamorphic belts in the Archaean. The WDC is characterized by mature continental sediment-dominated greenstone belts, as against the volcanic-dominated greenstone belts and granites in the EDC (Swaminath *et al.* 1976; Ramakrishnan 1988). The Dharwars are transitional southwards by increase in metamorphic grade (charnokitization) across an E–W-trending 30–60 km wide gneiss–granulite transition to the granulite terrain in the south. The extension of the Dharwar craton to the north is unknown, owing to the cover of Late Cretaceous (65 Ma) volcanic flows. These near-horizontal flows (Deccan trap) directly overlie the Archaean gneisses in most of the areas without any other substantial formation in between. A great scarp runs parallel to the west coast and is suggested to be a fault down throw on the western side (Pascoe 1964).

One of the Mid-Proterozoic episodes is localized basinal rifting with platform accumulations in depositional centres associated with extensional tectonic regimes. The Cuddapah type of depressions were formed in the already consolidated parts of the Indian shield. They probably occupied larger areas in addition to the present exposures. These sediments were later eroded, resulting in their complete removal from the elevated parts (Eremenko *et al.* 1969). Cuddapah basin sediments unconformably overlie the Peninsular gneiss, the eastern margin of which is faulted and overthrusted by Dharwar-type Archaean rocks. The Godavari graben is another Mid-Proterozoic intracratonic sedimentary basin formed under an extensional regime. Rifting activity was possibly initiated in this period along a pre-existing NW–SE-trending zone of weakness in the Dharwarian basement, and the rift developed by block faulting parallel to the bounding zone. The predominant sedimentation took place during the Gondwana period (Mahadevan 1994).

3 DATA AND METHODOLOGY

Five new broad-band stations namely GOA (15.48°N, 73.82°E), MNGR (12.87°N, 74.87°E), CUD (14.47°N, 78.77°E), UPL (17.29°N, 78.92°E) and KDM (17.58°N, 80.66°E) have become operative on the Indian shield (Fig. 1) since 1999. Stations GOA and MNGR lie on the WDC. Station UPL on the EDC lies very close to HYB (17.42°N, 78.55°E). Station CUD falls within the boundaries of the Proterozoic Cuddapah basin. Station KDM is in the Godavari graben, which separates the EDC from the Bhandara Craton to the northeast. For each of the recorded three-component seismograms, the signal-to-noise ratio (SNR) was computed based on the ratio of the *P*-coda energy and pre-*P*-onset noise. Only high SNR seismograms were subsequently used for computing the receiver functions.

The Z, N and E components of the seismograms are rotated into a ray coordinate system (L, Q, T), in which the L component is in the direction of the direct P phase, the Q component is in the direction of the SV phase and the T component is the third component in a right-handed coordinate system in the direction of the SH phase (Vinnik 1977). In order to optimize the decomposition of the wavefield into its P and SV components, we apply the methodology of Kennett (1991), which was adopted to the receiver function analysis by Bostock (1998). This technique allows a better separation of the direct P and scattered SV phases than the more commonly used rotation in the horizontal plane only, but requires knowledge of both the slowness of the incident wave and the near-surface velocity structure. The former can be computed using global velocity models such as IASP91 (Kennett & Engdahl 1991). The velocities are determined by minimizing the energy at $t = 0$ on the SV component (Saul *et al.* 2000).

Source-equalized SV and SH receiver functions are obtained by deconvolving the L component from the Q- and T-component seismograms, respectively, (Langston 1979; Owens *et al.* 1984). This is accomplished by simple spectral division in the frequency domain. A water-level stabilization, to avoid division instability and a low-pass Gaussian filter of 4 (or 2) Hz, to avoid high-frequency noise, are applied during deconvolution. In this work, we concentrate on examining the SV receiver functions,

as *SH* receiver functions, which contain information concerning lateral inhomogeneity and anisotropy, were not used due to inadequate azimuthal distribution of events with respect to the stations.

4 MOVEOUT CORRECTION

If the receiver functions are sorted according to slowness, the converted phases originating at different depths show different moveout slopes with respect to the *P* alignment, with the deeper conversions having larger moveouts. To compare directly the timing of the phases, these time differences have to be corrected. A slowness of 6.4 s deg^{-1} is taken as reference, which corresponds to an epicentral distance of 67° (Kind & Vinnik 1988). The times of receiver function samples from other epicentral distances are corrected to that of the reference trace on the basis of the IASP91 model. As the free surface reflected multiple phases have different moveouts compared with the direct conversions, it is necessary to perform the correction separately, for each wave type. This difference in moveout slopes provides a simple criterion to distinguish between converted and multiple phases. Receiver functions for the individual stations, moveout corrected for converted phases and averaged over narrow slowness bins (Fig. 2), clearly depict the Moho conversions (*Pms*) and corresponding *P* and *S* multiples (*Ppms* and *Psms*).

5 ESTIMATION OF POISSON'S RATIO AND ITS IMPORTANCE

Perhaps the most important factor in modelling receiver functions in terms of velocity and depth is the usage of the correct average crustal Poisson ratio (σ) . This can be obtained from the receiver functions themselves, provided good *Ppms* and *Psms* multiples of the converted *Pms* phase at the Moho are available. Since the crustal thickness cannot be accurately constrained from receiver function analysis without a Poisson ratio constraint, one may obtain a too high or a too low value for crustal thickness by assuming a default too low or too high Poisson ratio value. The assumption of an incorrect average crustal *P* velocity additionally affects the Moho depth (z_M) estimations. Fig. 3 demonstrates how *P* velocity and Poisson's ratio influence z_M estimates.

To have *a priori* control on σ below each station, we adapted the grid search approach of Zhu & Kanamori (2000). A σ–z_M pair, which best explains simultaneously the *Pms*, *Ppms* and *Psms* phases, emerges from a search over the σ–z_M space. The clear Moho multiples have resulted in well-constrained estimates of σ and z_M (as demonstrated from the low standard errors of estimations) beneath HYB, UPL and CUD (Fig. 4). For stations MNGR and GOA, this procedure was not successful due to the absence of clear multiples.

In the present Poisson's ratio determination procedure, we also obtain an estimate of crustal thickness, which, however, depends on the mean crustal *P* velocity used (Chevrot & van der Hilst 2000). A mean crustal *P* velocity of 6.5 km s^{-1}, obtained from wide-angle experiments (Kaila & Sain 1997), was used to arrive at the z_M values indicated for each station in Fig. 4. If it is not possible to compute the average crustal Poisson ratio from the receiver functions, one must use a 'proper' value of the same, preferably determined from some other sources. The estimates of crustal Poisson ratios for stations HYB, UPL and CUD, are in the range 0.23–0.25, and are likely to be representative of the EDC crust. In the WDC, for stations MNGR and GOA, no estimation of Poisson ratios was possible. However, we have earlier estimates (0.26) from two near-by stations on the DVP, namely PUNE and KARD and one estimate (0.25) from station TRVM on the southern granulite terrain (Kumar *et al.* 2001), all lying near the western margin. This shows that Poisson ratio values for the Indian shield, or at least for the western part, are quite similar irrespective of the intra-Peninsular geological divisions, with all values falling between 0.24 and 0.26. We therefore modelled the crust below MNGR and GOA by constraining the Poisson ratio (0.25) from these estimates.

6 MODELLING OF RECEIVER FUNCTIONS

Assuming an average crustal *P* velocity of 6.5 km s^{-1}, a Poisson ratio of 0.25 results in a crustal thickness estimate of 43 km corresponding to a *Pms* time of 5.0 s (an average for WDC). A 4.0 s *Pms* time (average for EDC) similarly produces a z_M estimate of 34 km, indicating a substantially (about 9 km) thinner crust compared with the WDC crustal thickness. The z_M values have been later refined by actually using the average velocities computed from the respective velocity models, developed from forward modelling. The above rule-of-thumb estimates of crustal thickness from delay time information alone, need to be refined with amplitude modelling of the receiver functions. For this, the phases that are most conspicuous across the whole slowness range, have been identified on the stacked receiver functions. Later, drawing constraints from the Poisson ratio estimates, these phases were modelled. For stations GOA and MNGR, we preferred to model the observed receiver functions computed using a low-pass Gaussian filter of 2 Hz, since the data from these stations had significantly more high-frequency noise.

We adopted a forward modelling (Fig. 5) strategy using plane-wave synthetic seismograms (Kind *et al.* 1995). These were computed for an angle of incidence averaged over all epicentral distances of the observed traces. The synthetic traces are rotated and deconvolved in the same manner as the observed traces for making meaningful comparisons with the observed receiver functions. In the modelling of receiver functions, one can usually only model the velocity contrasts across the discontinuities. Thus the absolute velocities remain uncertain, unless some other constraints are imposed.

7 RESULTS AND DISCUSSION

Usually, the most noticeable phase in receiver functions is the *P*–*S* converted phase (*Pms*) at the Moho (Fig. 2). Its delay time gives a first hand estimate of the crustal thickness. A cursory look at the sections reveals that the crust below all the stations on the Dharwar craton is simple with a sharp Moho phase but devoid of any prominent intracrustal conversions. However, stations GOA (5.2 s) and MNGR (4.9 s) have considerably larger delay times compared with stations HYB (3.9 s), UPL (3.7 s) and CUD (4.1 s). The former stations are situated on the WDC, whereas the latter are on the EDC. Station KDM located on sediments of the Godavari graben in contrast exhibits very different receiver functions devoid of strong Moho multiples that are characteristic of most of the cratonic stations. Besides an early conversion from the basement and a weak Moho conversion at 5.1 s, it is characterized by a strong mid-crustal phase at 2.8 s.

As already stated, the *S*-velocity models (Fig. 5) are based on forward modelling, which has considered only consistent and significant phases seen on the receiver function sections (Fig. 2), while ignoring insignificant kinks in the traces. The matches between the observed and synthetic receiver functions vary from very good to

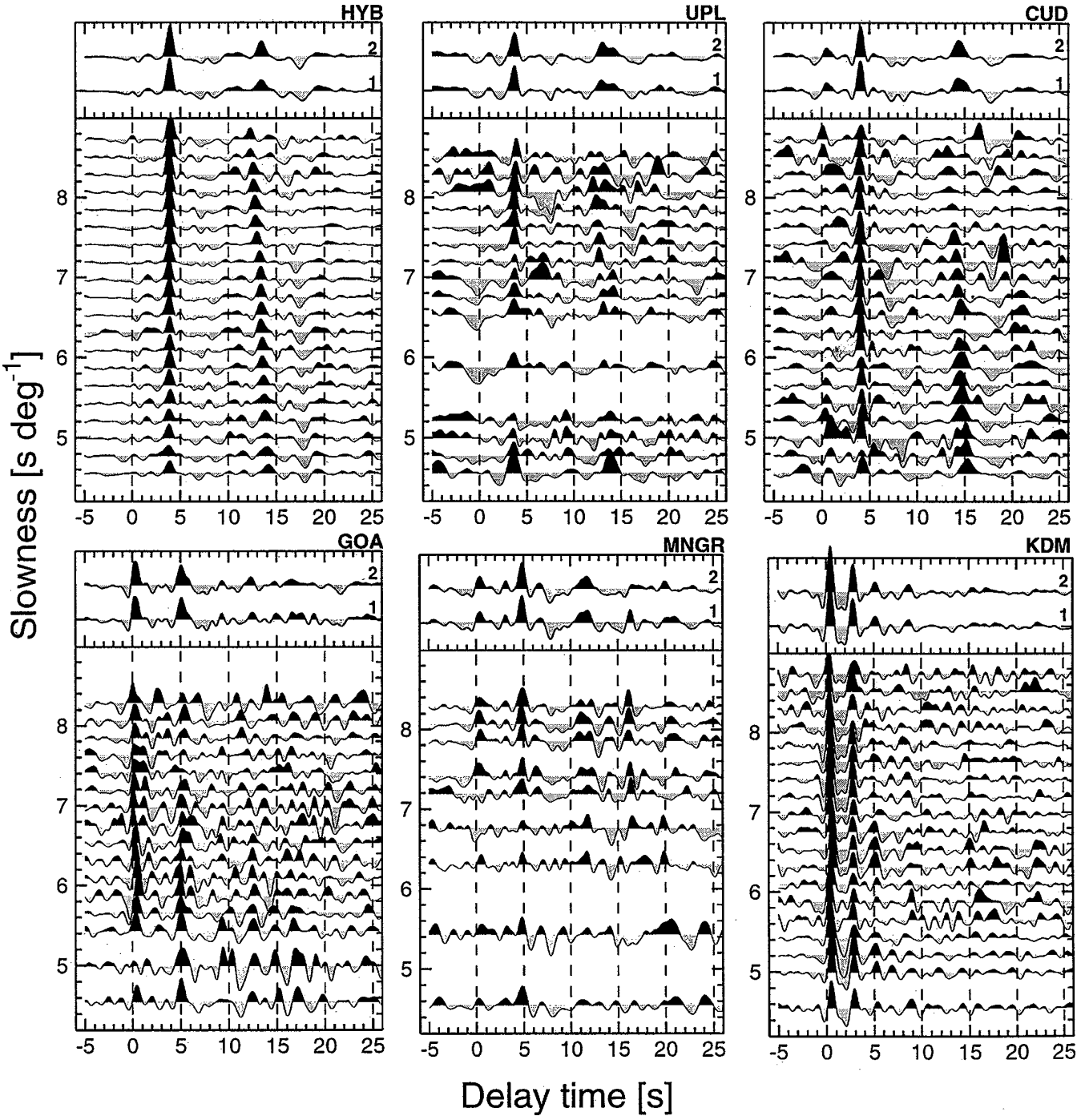

Figure 2. Receiver functions for the stations used in this study, moveout-corrected for converted waves and averaged over narrow slowness bins. On the top, the corresponding summation traces (1) are shown. Also shown (2) are the summation traces for the receiver functions moveout-corrected for the first multiples (corresponding slowness sections not shown). Note that conversions and multiples have enhanced amplitudes on 1 and 2, respectively.

satisfactory. The model for station HYB with the largest amount of available data was taken from Saul *et al.* (2000). The nearby station UPL with far fewer events has an almost identical velocity structure, but without a good match of the amplitudes of the multiples, due to lower SNR. The data from station CUD could also be matched very well by the synthetics. For this station an *S*-velocity model largely similar to that for HYB and UPL, save for the top few kilometres (the sedimentary part), has been obtained. The data from CUD show a deeper Moho (36 km), compared with HYB and UPL (33 and 32 km, respectively), but broadly these stations can be grouped together, exhibiting a thin and transparent EDC crust. This possibly indicates the absence of intense reworking or rejuvenation of the crust during basin formation.

The data from station KDM with a *Pms* conversion time for the Moho of 5.1 s were not modelled due to the large conversion from the basement. However, the Moho conversion time is in conformity with the Moho depth of 42 km reported by Kaila *et al.* (1990a) from wide-angle studies. The receiver functions definitely indicate a very

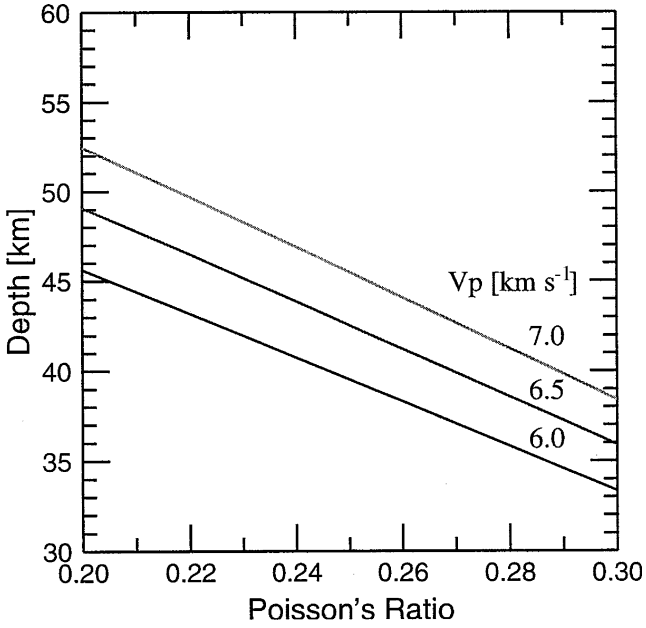

Figure 3. Variation in Moho depths, for a 5 s delay time over a range of Poisson ratios. Curves for three average crustal *P* velocities (*Vp*) are shown.

different type of crust compared with the adjacent EDC crust. At station KDM, besides the conversion from the base of the graben, a strong intracrustal conversion is seen. This boundary may correspond to the top of a high-velocity mafic material (rift pillow), which intruded the crust from the upper mantle during the extensional phase of rift formation. Evidence for such rift pillows has been found in many parts of the globe, such as the Cambay basin in western India and the Kenya rift in eastern Africa (Kaila *et al.* 1990b; Mechie *et al.* 1997).

For stations GOA and MNGR, we used a Poisson ratio value of 0.25 (see above). In the forward modelling of receiver functions for these stations, although we could match the converted phases very well, the match for multiples, which are in any case not well observed, is not satisfactory. The models developed show that both the WDC stations, lying near the west coast, are characterized by a thick (>40 km) crust and a gradational Moho resulting from a lack of multiples. The lack of coherent multiples and broadening of the Moho conversion could be attributed to a dipping Moho. Weaker intracrustal phases, observed at variable times for these stations, indicate a WDC crustal character that is more complicated than that of the EDC. It is, however, possible that the multiple of one such phase from a shallow boundary has interfered with the *Pms* conversion from the Moho, contributing to broadening of the observed pulse. Furthermore, the two western coastal stations may not be fully representative of the entire WDC. The WDC crust may vary regionally, and may even become thicker as one goes inland.

Our results indicate that the Archaean Dharwar crust has a uniformly low average Poisson ratio of about 0.25, and is simpler than the adjacent Proterozoic crusts of the Eastern Ghat Mobile Belt or Narmada-Son regions, which are in general thicker and more complex (Kumar *et al.* 2001). Mineralogically, the low Poisson ratio of the Dharwar crust would signify an overall abundance of quartz in the crustal material (Tarkov & Vavakin 1982; Christensen 1996). Alternatively, it is possible that the Dharwar crust is divided into a more felsic upper crust with a Poisson ratio lower than 0.25 and a mafic lower crust with a correspondingly higher Poisson ratio. Such a partitioning need not necessarily require a strong mid-crustal *S*-velocity contrast and may manifest as a contrast in *P* velocities only. This possibility gains support from the results of earlier wide-angle experiments in the Dharwar craton, which indicated the presence of a mid-crustal boundary at about 23 km depth in the *P*-velocity models (Kaila *et al.* 1979; Sarkar *et al.* 2001).

In any case, a clear distinction exists in crustal structure between the eastern and western Dharwar cratons. The EDC crust (average thickness 34 km) with a sharper Moho is thinner and more transparent than the WDC crust (average thickness 41 km), though the average crustal *S* velocities are similar (3.6–3.8 km s^{-1}). Thus the difference in crustal thickness is about 7 km. The difference could be even more, since all the WDC stations incidentally lie near the western coast, where the continental crust is expected to thin in the transition to oceanic crust. Alternatively, the continent to ocean transition takes place further west, and a continental block, down-thrown along a west coast fault, exists under the seas.

Sarkar *et al.* (2001), analysing the refraction/wide-angle reflection traveltime data of the WDC part of an E–W coast-to-coast (Kavali-Udipi) profile, reported a Moho depth of about 39–40 km. Reddy *et al.* (2000) observed that this value for the WDC crust was somewhat higher than that for the EDC crust (about 36–37 km). The WDC crustal thickness is significantly more than the average value (35 km) indicated in the CRUST 5.1 model of Mooney *et al.* (1998) for the south Indian shield. For the DVP, Kaila *et al.* (1981) presented

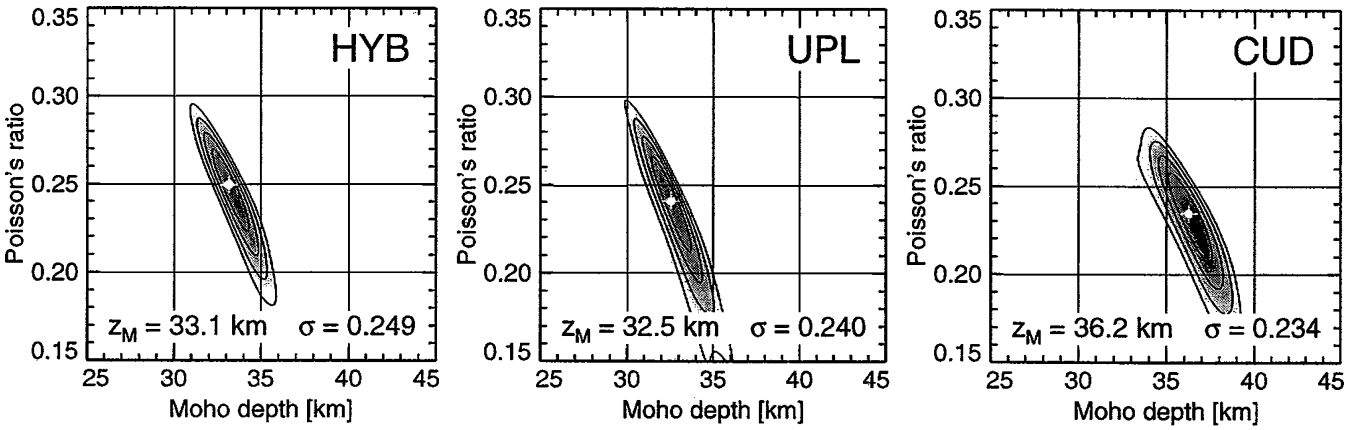

Figure 4. Determination of the Poisson ratio (σ) for three EDC stations. Standard errors in the Poisson ratio estimates are 0.01 for HYB and 0.02 for UPL and CUD. Uncertainties in Moho depth estimates are of the order of 2 km.

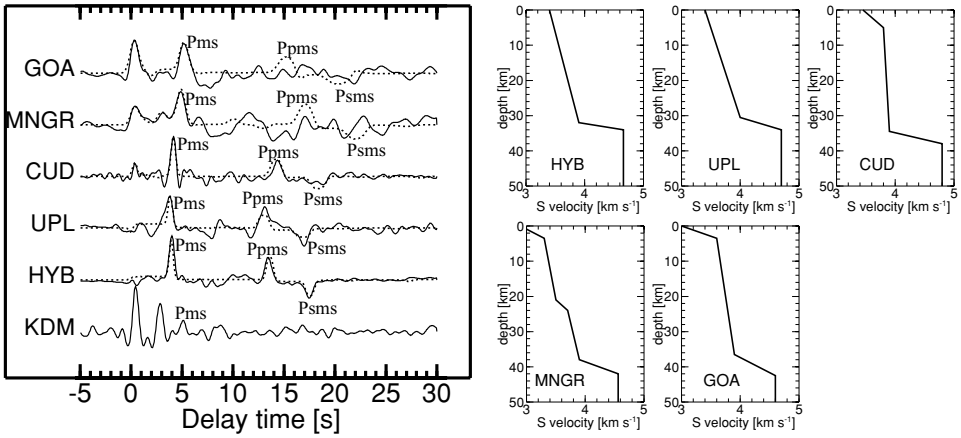

Figure 5. Comparison of observed (solid line) and synthetic (dotted line) *SV* receiver functions for various stations. *S*-velocity models corresponding to the synthetic traces are shown on the right. The result for HYB was taken from Saul *et al.* (2000).

a Moho picture based on the data from two refraction/wide-angle reflection profiles. This picture showed a Moho up-dipping from 37 to 30 km towards the western coast. Krishna *et al.* (1999) from modelling of aftershock seismograms reported a crustal thickness of about 37 km for the Latur and Koyna epicentral regions of the DVP. These values from the DVP are rather more representative of distant EDC than of the thicker WDC. Also, a crustal thickness of 36.5 km for the DVP was obtained for the KARD station (Kumar *et al.* 2001) close to one of the DSS profiles. The present results, obtained as 'spot' values (as against averaged values in refraction studies) on different parts of the Dharwar craton, confirm the differences in crustal thickness between the WDC and the EDC, a hypothesis made by Swaminath & Ramakrishnan (1981) on geological considerations.

8 CONCLUSIONS

(1) The shear wave structure of the entire Dharwar crust is largely simple, devoid of major intracrustal discontinuities, and shows a low Poisson ratio. Thereby, no distinct separation exists in terms of upper and lower crust. On the whole, the Dharwar crust is thinner and less complex than its adjacent Proterozoic crust.

(2) The WDC crust is distinctly thicker than the EDC crust by at least 7 km. Also, the WDC Moho is more gradational, compared with its eastern counterpart. Though the WDC crust is less transparent than the EDC crust, no substantial differences in average crustal *S* velocities were found.

(3) Formation of the Cuddapah basin did not significantly alter the crustal configuration, as testified by thin and simple EDC crust underneath.

(4) From the large crustal thickness near the WDC coast, it appears that the Indian continental margin is further off the western coast. A possible west coast fault must have down-thrown the western block of continental crust, which is submerged under the sea.

(5) The crust below the DVP is more akin to the EDC crust in terms of thickness. This suggests that WDC does not extend much to the north underneath the trap cover.

(6) The crustal structure underneath the Godavari graben is significantly different from the neighbouring EDC and also from the WDC. Signatures of a deeper Moho, compared with the EDC, and a sharp intracrustal boundary are clearly visible on receiver functions. The intracrustal boundary corresponds to the top of a rift pillow, such as is found under many rifts globally.

ACKNOWLEDGMENTS

This work has been performed under a CSIR-DLR collaborative scientific project between GFZ and NGRI. We are especially grateful to Dr H. K. Gupta and Professor S. J. Duda for their involvement in the project. Dr Gupta has also reviewed the paper. Dr James Mechie has gone through the manuscript critically. J. Saul has also been supported by the Deutsche Forschungsgemeinshaft. The India Meteorological Department has made the available a part of the data used. All the help is gratefully acknowledged.

REFERENCES

Bostock, M.G., 1998. Mantle stratigraphy and evolution of the Slave province, *J. geophys. Res.,* **103,** 21 183–21 200.

Chevrot, S. & van der Hilst, R.D., 2000. The Poisson ratio of the Australian crust: geological and geophysical implications, *Earth planet. Sci. Lett.,* **183,** 121–132.

Christensen, N.I., 1996. Poisson's ratio and crustal seismology, *J. geophys. Res.,* **101,** 3139–3156.

Eremenko, N.A. *et al.*, 1969. Tectonic map of India by Oil and Natural Gas Commission—principals of preparation, *Bull. Oil Nat. Gas Comm.,* **6,** 1–11.

Goodwin, A.M., 1996. *Principles of Precambrian Geology,* p. 327, Academic, London.

Kaila, K.L. & Krishna, V.G., 1992. Deep seismic sounding studies in India and major discoveries, *Curr. Sci.,* **62,** 117–154.

Kaila, K.L. & Sain, K., 1997. Variation of crustal velocity structure in India determined from DSS studies and their implication on regional tectonics, *J. Geol. Soc. Ind.,* **49,** 395–407.

Kaila, K.L., Murthy, P.R.K., Rao, V.K. & Kharetchko, G.E., 1981. Crustal structure from deep seismic soundings along the Koyna II (Kelsi-Loni) profile in the Deccan trap area, India, *Tectonophysics,* **73,** 365–384.

Kaila, K.L., Murthy, P.R.K., Rao, V.K. & Venkateshwarlu, N., 1990a. Deep seismic sounding in the Godavari Graben and Godavari (Coastal) Basin, *Tectonophysics,* **173,** 307–317.

Kaila, K.L., Tewari, H.C., Krishna, V.G., Dixit, M.M., Sarkar D. & Reddy, M.S., 1990b. Deep seismic sounding studies in the north Cambay and Sanchor basins, *Geophys. J. Int.,* **103,** 621–637.

Kaila, K.L. *et al.*, 1979. Crustal structure along Kavali-Udipi profile in the Indian peninsular shield from deep seismic sounding, *J. Geol. Soc. Ind.,* **20,** 307–333.

Kennett, B.L.N., 1991. The removal of free surface interactions from three-component seismograms, *Geophys. J. Int.,* **104,** 153–163.

Kennett, B.L.N. & Engdahl, E.R., 1991. Travel times for global earthquake location and phase identification, *Geophys. J. Int.,* **105,** 429–465.

Kind, R. & Vinnik, L., 1988. The upper mantle discontinuities underneath the GRF array from *P* to *S* converted phases, *J. Geophys.,* **62,** 138–147.

Kind, R., Kosarev, G. & Petersen, N., 1995. Receiver functions at the stations of the German Regional Seismic Network (GRSN), *Geophys. J. Int.,* **121,** 191–202.

Krishna, V.G., Rao, C.V.R.K., Gupta, H.K., Sarkar, D. & Baumbach, M., 1999. Crustal seismic velocity structure in the epicentral region of Latur earthquake (September 29, 1993), Southern India: inferences from modeling of the aftershock seismograms, *Tectonophysics,* **304,** pp. 241–255.

Kumar, M.R., Saul, J., Sarkar, D., Kind, R. & Shukla, A.K., 2001. Crustal structure of the Indian shield: new constraints from teleseismic receiver functions, *Geophys. Res. Lett.,* **28,** 1339–1342.

Langston, C.A., 1979. Structure under Mount Rainier, Washington, inferred from teleseismic body waves, *J. geophys. Res.,* **84,** 4749–4762.

Mahadevan, T.M., 1994. Deep continental structure of India: a review, *Geol. Soc. Ind. Mem. Bangalore (India)* **28,** 569.

Mechie, J., Keller, G.R., Prodehl, C., Khan, M.A. & Gaciri, S.J., 1997. A model for the structure, composition and evolution of the Kenyan rift, *Tectonophysics,* **278,** 95–119.

Mooney, W.D., Laske, G. & Guy Masters, T., 1998. CRUST 5.1: a global crustal model at $5^\circ \times 5^\circ$, *J.Geophys. Res.,* **103,** 727–747.

Naqvi, S.M. & Rogers, J.J.W., 1996. *Precambrian Geology of India,* Clarendon, New York.

Owens, T.J., Zandt, G. & Taylor, S.R., 1984. Seismic evidence for an ancient rift beneath the Cumberland Plateau, Tennessee: a detailed analysis of broadband teleseismic *P* waveforms, *J. geophys. Res.,* **89,** 7783–7795.

Pascoe, E.H., 1964. *A Manual of Geology of India and Burma,* vol. 3, pp. 1345–2130, Publ. Govt. of India, Delhi.

Ramakrishnan, M., 1988. Tectonic evolution of the Archean high grade terrain of south India, *J. Geol. Soc. Ind.,* **31,** 118–119.

Reddy, P.R., Venkateswarulu, N., Koteswara Rao, P. & Prasad, A.S.S.S.R.S., 1999. Crustal structure of peninsular shield, India from DSS studies, *Curr. Sci.,* **77,** 1606–1611.

Reddy, P.R., Chandrakala, K. & Sridhar, A.R., 2000. Crustal velocity structure of the Dharwar Craton, India, *J. Geol. Soc. Ind.,* **55,** 381–386.

Sarkar, D., Chandrakala, K., Padmavathi Devi, P., Sridhar, A.R., Sain, K. & Reddy, P.R., 2001. Crustal velocity structure of western Dharwar craton, south India, *J. Geodyn.,* **31,** 227–241.

Saul, J., Ravi Kumar, M. & Sarkar, D., 2000. Lithospheric and upper mantle structure of the Indian shield using teleseismic receiver functions, *Geophys. Res. Lett.,* **27,** 2357–2360.

Swaminath, J. & Ramakrishnan, M., 1981. Early Precambrian supracrustals of southern Karnataka, *Mem. Geol. Surv. Ind.,* **112,** 350.

Swaminath, J., Ramakrishnan, M. & Viswanathan, M.N., 1976. Dharwar stratigraphic model and Karnataka craton evolution, *Rec. Geol. Surv. Ind.,* **107,** 149–179.

Tarkov, A.P. & Vavakin, V.V., 1982. Poisson's ratio behaviour in crystalline rocks: application to study the Earth's interior, *Phys. Earth planet. Inter.,* **29,** 24–29.

Vinnik, L.P., 1977. Detection of waves converted from *P* to *SV* in the mantle, *Phys. Earth planet. Inter.,* **15,** 294–303.

Zhu, L. & Kanamori, H., 2000. Moho depth variation in southern California from teleseismic receiver functions, *J. geophys. Res.,* **105,** 2969–2980.